

## **A COMPLETELY REMOTE SENSING APPROACH TO MONITORING RESERVOIRS WATER VOLUME**

*R. Abileah<sup>1</sup>, S. Vignudelli<sup>2</sup>, and A. Scozzari<sup>3</sup>*

<sup>1</sup> jOmegak, San Carlos CA, USA, [E-mail: abileah@omegak.com](mailto:abileah@omegak.com)

<sup>2</sup> CNR – Istituto di Biofisica, [E-mail: vignudelli@pi.ibf.cnr.it](mailto:vignudelli@pi.ibf.cnr.it)

<sup>3</sup> CNR - Istituto di Geoscienze e Georisorse, [E-mail: a.scozzari@igg.cnr.it](mailto:a.scozzari@igg.cnr.it)

### **ABSTRACT**

*Measurements of volume variations in water reservoirs provide information critical to climate change and resource monitoring, especially in the context of the growing challenges for the management of the resource. However, many reservoirs are located in remote regions, which make difficult the deployment and regular maintenance of traditional in-situ measurement systems; also, the new perspective of free and public satellite data is encouraging new monitoring opportunities in areas which were not possible before. All of these factors make satellite remote sensing an attractive tool for a global monitoring of reservoirs. In particular, remote sensing resources that are freely available nowadays represent a great opportunity to support the study and monitoring of hydrological and hydraulic processes. In this paper we describe the fusion of two such freely available Earth orbiting satellite data: Landsat optical images (preprocessed to Level 1) and radar altimeters from several satellites (processed into water levels), to remotely monitor reservoir water capacity.*

**Keywords:** *Remote sensing, Landsat, Radar altimetry, Lakes, Water volume*

### **1. INTRODUCTION**

The authors are specialists in remote sensing science, not in hydrology and especially not in reservoir monitoring. The first author (Abileah) has worked in other applications of imaging satellites. The second author (Vignudelli) is a specialist in radar altimetry (Vignudelli et al. [1]). Our interest in reservoir monitoring was inspired by Jens Liebe's PhD thesis (Liebe [2]) and later with the voluminous report (UNESCO [3]) of the Small Reservoir Project. These references introduced a methodology for measuring water capacity of reservoirs using images from Earth orbiting satellites combining space based imagery with in situ derived reservoir bathymetry. After reading these references we realized that we could replace the in situ bathymetry with information derived from radar altimetry observations. This eliminates the need for surveying on the ground and provides the reservoir capacity entirely based on Earth orbiting satellite data.

We begin with a temporal sequence of Landsat imagery and radar altimetry, both covering the same time interval. Each Landsat image is an instance of the water body characterized by a different water level. The instantaneous shoreline defines a depth contour. The corresponding height is estimated from the radar altimetry

data close in time to the optical image. A temporal sequence of such paired optical and radar altimetry thus provides a bathymetric profile which can in turn be transformed into frustum volume sections.

We demonstrate the technique with imagery and radar altimetry data over Lake Nasser for the period 1998-2004. We also show water level fluctuations in the Toshka basin during the period when the Toshka lakes were first created by diversion of Lake Nasser water.

There are also useful byproducts of our method. First, the method provides a remotely sensed bathymetry, which may be useful for navigating the shallow nearshore waters. Second, once a reservoir is calibrated (to be explained) the method provides a more accurate water level gauge than radar altimetry alone.

## 2. METHOD

Two observation time series are used: first, the water surface areas,  $A(t_n)$ , for  $n = 1, 2, \dots, N$ , LANDSAT, as described in Appendix I. Second, water levels,  $L(\tau_m)$ ,  $m=1, 2, \dots, M$ , from satellite radar altimeters, described in more detail in Appendix II. Ideally the two time series would be precisely time synchronized, but this is rarely the case. Both satellite systems are nadir looking and revisit the same location on the Earth surface at regular intervals typically 2-3 times per month (see Appendices I and II for specifics), but not on exactly the same days.

One of the two time series needs to be interpolated to the times of the other. For interpolation the time series must be critically sampled, which is another way of saying that a *sinc* interpolation between samples will provide accurate inter-sample observations. If the data is well over-sampled, linear interpolation can be used. In some cases it may be sufficient to use the pair of observations closest in dates, which is equivalent to nearest-neighbor interpolation.

In lakes, rivers, and reservoirs, the water levels usually follow annual cycles. The radar altimetry satellites sample at various intervals (see Appendix II). If we combine data of two or three radar altimeters the sampling rate may be as much as 4/month. So in general it can be assumed that the radar altimeter time series over-samples the water level variations, and we are safe to interpolate the series. It should be noted that this is not the true for bodies of water influenced by diurnal and semidiurnal tide cycles.

Landsat image intervals can be as small as 16-day but are generally greater due to clouds, haze, and other operational constraints. In some parts of the world (but not Egypt) clouds can obstruct views for several consecutive months. Given all considerations one generally finds that usable Landsat images occur at frequencies  $\leq 1/$  month. We therefore always interpolate the radar altimetry data to the times of Landsat images.  $L(t_n)$ , is the interpolated version of  $L(\tau_m)$ , matching the Landsat time series point for point.

The volume of a pyramidal frustum was derived 2000 years ago by Heron (Greek mathematician, native of Alexandria, 10-70 AD) as follows:

$$AV = \frac{L_1 - L_2}{3} (A_1 + A_2 + A_1 A_2)$$

where  $L_1$  and  $L_2$  are two water levels with corresponding surface areas  $A_1$  and  $A_2$ . Even after 2000 years this is still the basic formula used by limnologists to compute the volume of lakes (Taube [4]).

The equation applies when the area increases linearly with change in water level. This assumption is valid for small intervals in water level but not necessarily true over large changes in water level. The usual practice is to sum a series of consecutive frustums were the approximation is valid.

One way to apply Heron's formula to the Landsat-Radar Altimeter time series is to let  $A'$  be the area measurements sorted in ascending order, and  $L'$  be the corresponding levels, then  $AV_{12}$  is computed from the first sorted observation pair,  $AV_{23}$  from the second pair, and so forth. Summing all the incremental volumes provides the total capacity.

Another and potentially more precise volume may be derived as follows. Fit a polynomial function,  $F$ , using a robust fitting of the scatter between the  $A$  and  $L$  observations. Robust means that the fit is desensitized to large outliers. The fitting process should include a constraint that  $F(L)$  is monotonically increasing (since any increase in water level must be accompanied by increase in water area). We then have reduced noisy time series data points into a smooth continuous functional relationship,  $A=F(L)$  and volume can be obtained by simply integrating,

$$V_{12} = \int_{L_1} F(L) dL$$

where  $(L_1, L_2)$  is the span of observed water levels. When the span covers dry bed to maximum capacity the total volume and various increments can be computed reliably. If the full range of water levels cannot be observed (i.e., the reservoir is always partially filled) the approach outlined here is useful for the upper most layer and the leaves the bottom portion unknown.

Bathymetry is a byproduct. Each Landsat image provides the outline of the shoreline at a corresponding water level. A series of area-level data then define a series of such contour lines, hence a detailed bathymetry. This idea was demonstrated earlier using space-based SAR ([Mason [5]) and optical (Yamano [6]) imaging satellites combined with water level data from in situ tidal gauges. Here we have a completely remote sensing approach to bathymetry.

Another byproduct is the calibration for a remote sensing water level or tidal gauge. Once the  $F(L)$  relationship is established for a given area future Landsat images can be used to track water levels independently of radar altimetry. This could include backtracking to earlier times when Landsat was operational but radar altimeters were not. Now and into the future "Landsat water level gauges" can provide greater water level accuracy on coastal areas, although this is yet to be confirmed experimentally.

### 3. TESTING THE METHOD

The ideal way to verify this method would be a test on a reservoir where there is both long-term satellite coverage and simultaneous ground truth obtained by traditional sonar bathymetry and water level gauges. Furthermore the ideal test case would have the satellite observations span a period of time when the reservoir levels range from the minimum (dry bed) to full capacity. The authors are planning such a test in the near future but at this time we can report on a test without such ground truth. The verification of the method is then established by showing repeatable results. This is not as good as ground truth but still useful.

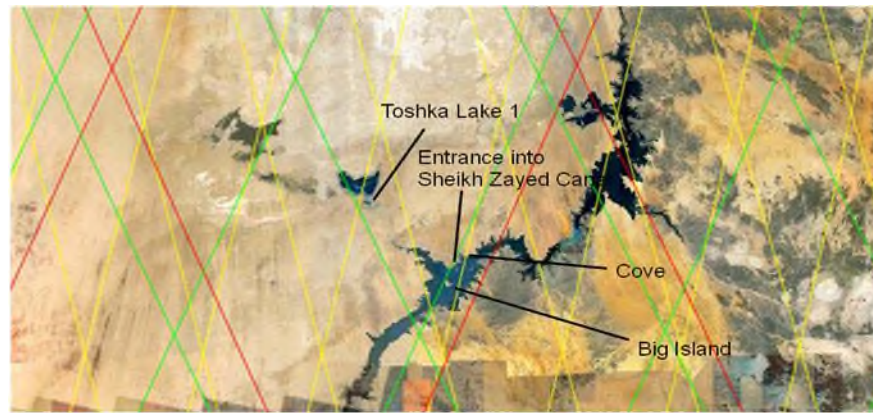


Fig. 1 The region of investigation with the areas selected for testing the method. The radar altimetry ground track coverage is also showed (TOPEX/Poseidon and Jason 1/2, red; Geosat Follow-On, green; Envisat, yellow)

### 3.1 Study Area

The general area of the test was in Lake Nasser (Figure 1). The color lines shows the nadir paths of several radar altimeters. Note that Lake Nasser is well sampled at several different point by all radar altimeters. The frequency of satellite altimetry is thus very high and certainly sufficient to track the seasonal water level variations. For this study we selected smaller areas within the larger lake and treated them as individual "reservoirs." They are: (1) an area centered on the entrance into the Sheikh Zayed Canal that drains Lake Nasser water into the Toshka depression ( $22^{\circ}38'N$ ,  $31^{\circ}51'E$ ), (2) the water surrounding an unnamed island in the middle that we will refer to simply as the "Big Island" ( $22^{\circ}29'N$ ,  $31^{\circ}48'E$ ), and (3) the area referred to as the "Cove" ( $22^{\circ}40'N$ ,  $31^{\circ}52'E$ ). Another area for this study is one of the nearby man-made Toshka Lakes (see Ismail [7] for an excellent account of these lakes). We report our observations of water area for "Lake 1" in Figure 1 ( $23^{\circ}0'N$ ,  $31^{\circ}19'E$ ).

### 3.2 The data time period

For the radar altimetry data we used two online databases:

- 1) USDA's TOPEX/Poseidon and Jason satellites data base (see at <http://www.pecad.fas.usda.gov/lakes/images/lake0331.TPJO.1.smooth.txt>)
- 2) LEGOS's Hydroweb data base (see at [http://www.legos.obsmp.fr/en/soa/hydrologie/hydroweb/StationsVirtuelles/SV\\_Lakes/Nasser.html](http://www.legos.obsmp.fr/en/soa/hydrologie/hydroweb/StationsVirtuelles/SV_Lakes/Nasser.html)). Major details about these data bases are reported in Appendix II. The two data sets were combined into one time series of water level (Figure 2) spanning over two decades (1992 to present). In the combined series over 80% of the sample intervals are  $\leq 10$  days. As mentioned earlier, the sampling is more than adequate to interpolate to Landsat dates.

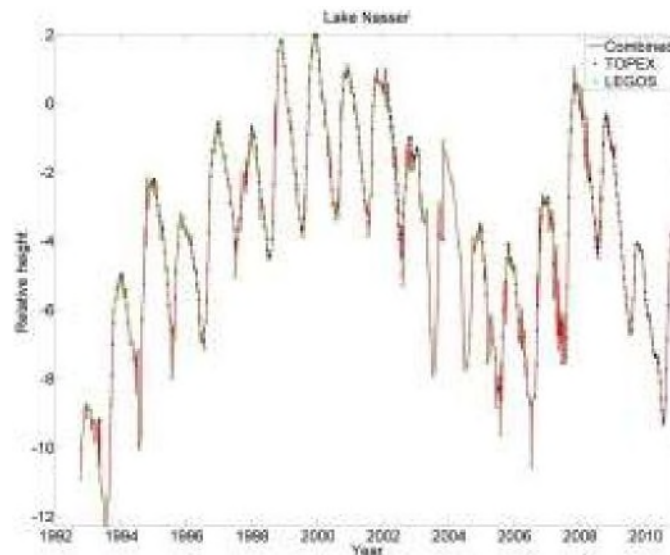


**Fig. 2 Relative water height variability of Lake Nasser from combined radar altimetry**

LANDSAT 4 images of Lake Nasser begin in 1984. LANDSATs 5 and 7 come into operation afterwards and are still operational today. The combination should in theory provide a continuous coverage from 1984 to the present. This is true in some area of the world, notably over the USA, but unfortunately not over Egypt where there are notable gaps. Specifically Lake Nasser is covered up to 1992, then not at all in 1992-1997. Landsat 5 resumed imaging the area in 1998, and Landsat 7 begins in 1999. Unfortunately Landsat 7 suffered a malfunction in early 2003 resulting in loss of 22% of the image scan lines (see at [http://landsat.usgs.gov/products\\_slcoffbackground.php](http://landsat.usgs.gov/products_slcoffbackground.php)).

Many users of Landsat 7 use fill-in algorithms to repair post 2003 Landsat 7 imagery but we decided that such fill-in was not appropriate for this study. Hence we do not use post 2003 Landsat 7 data. Landsat 5 continues to provide excellent imagery to this day but for some reason does not cover Lake Nasser after 2004. Perhaps the Landsat operators decided the Landsat 7 provided sufficient revisits of this area. In taking all the above into consideration we are left with the period 1998-2004 where good Landsat imagery is available and overlaps the radar altimetry data.

### 3.3 Lake Nasser results

During the 1998-2004 period the water level of Lake Nasser varies over a range of 10 m. The water capacity derived by our method thus applies to this top 10-m layer. We do not attempt to extrapolate beyond the observational range.

What follows discusses the results for the first "reservoir," the area centered on the Sheikh Zayed Canal entrance, bounded by an actual shoreline and artificial straight line over the water, as indicated in Figure 3. The entrance into the Sheikh Zayed Canal is the wrench shaped feature in the center. Figure 3 also shows the bathymetric contours derived in the same analysis, as will be explained later.

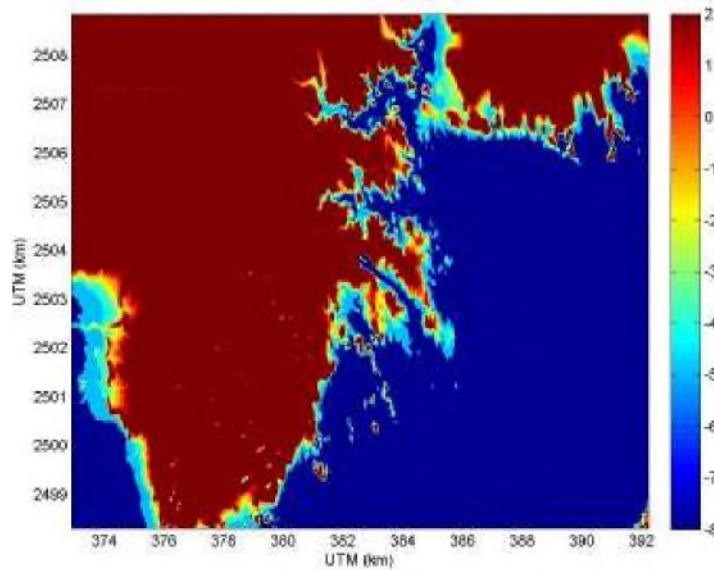


Fig. 3 Canal inlet bathymetry (m)

The computational steps leading to estimating the water volume are shown in Figure 4. Figure 4 top left panel shows the scatter of observation data with the radar altimetry on the x-axis and corresponding Landsat derived water areas on the y-axis. The least square fit of a polynomial equation describes the functional relationship,  $F$ , which is plotted on the graph. Most of the data is close to the fitted function but a few are far off. These turn out to be images contaminated with clouds or significant haze. We could have applied algorithms that detect clouds beforehand and not included them, but it is easier to let the  $F$  fit do the job of identifying the outliers. Large outliers are excluded in a second iteration which is shown in upper right panel.

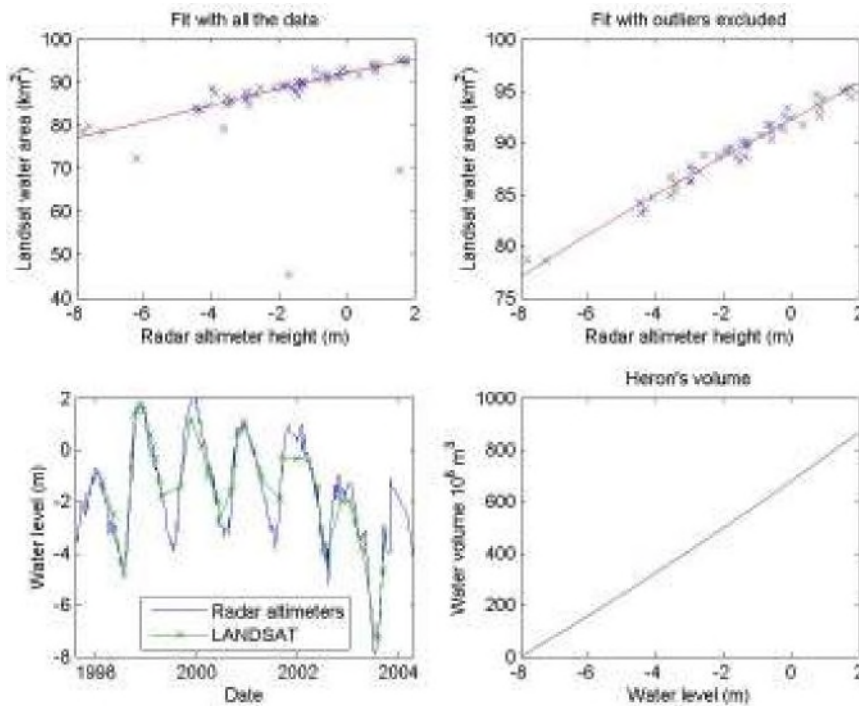


Fig. 4 Canal inlet area inferred from Landsat vs. radar altimetry height (upper panels) and water volume from Heron's formula (lower right panel)

The scatter that remain about the best fit is small but indicate some error in the observation data. This is of course to be expected. We believe (but have yet to prove rigorously) that the water area is the more precise data. Most of the noise is in the radar altimetry levels. The data suggests that the rms radar altimetry errors are 5-10 cm. Not bad, even for an in situ gauge. But the F(A) smoothes out these errors so that the final water level rms is even smaller.

We use the second iteration fit to plot the Landsat based water levels and compare them with radar altimetry in the bottom left panel. The agreement is excellent.

In the bottom right panel is the water volume as determined with the integral form of Heron's volume. The volume is relative to the lowest level over the observation period, not the actual full volume. It accurately measures the volume of water in the annual cyclical pattern.

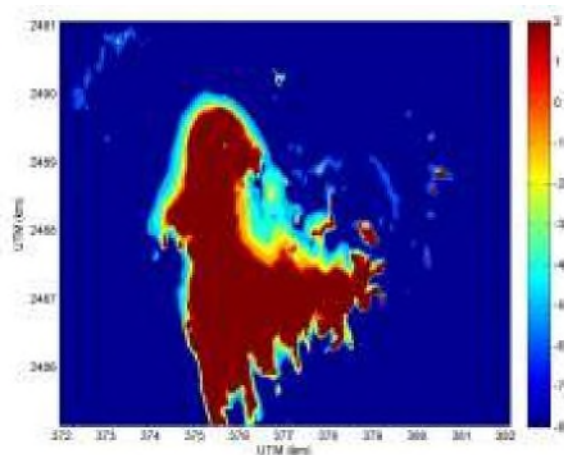


Fig. 5 Island bathymetry (m)

The second artificial reservoir is the vicinity of the Big Island, with similar results shown in Figures 5-6. In the Big Island case the artificial reservoir bounds are a square area of water, as shown in Figure 5.

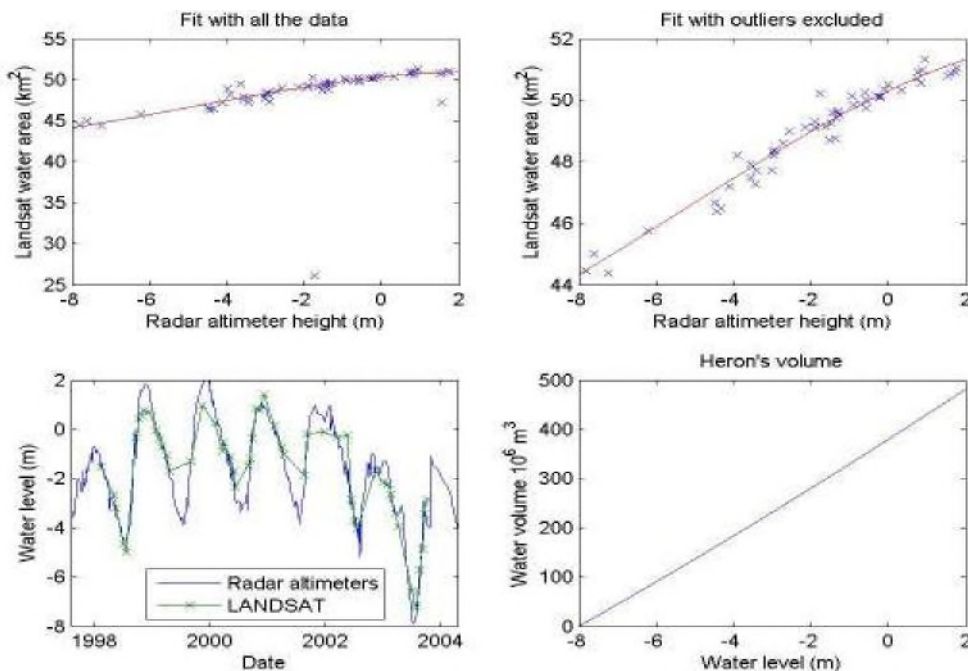


Fig. 6 Island area inferred from Landsat vs. radar altimetry height (upper panels) and water volume from Heron's formula (lower right panel)

The variability in water area comes from the island in the center. This demonstrates that an island is as useful to this method as an enclosed water body. For example, an island in the middle of an ocean could be used as a remote water gauge once the  $F(A)$  relationship has been established for that island.

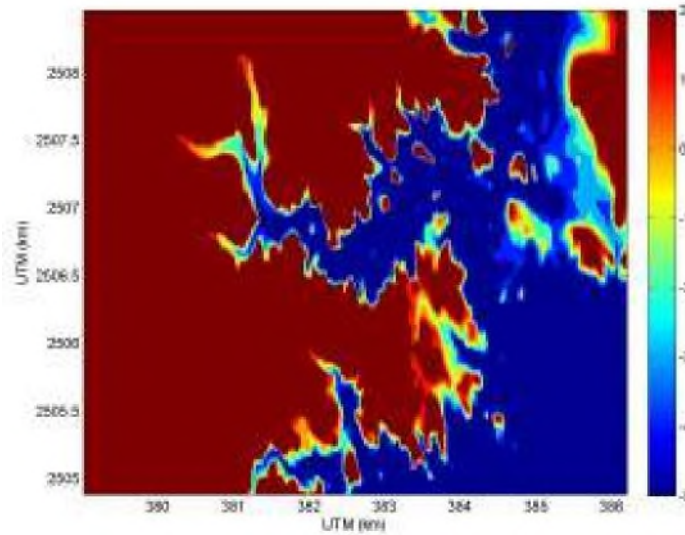


Fig. 8 Cove bathymetry (m)

The third artificial reservoir is the Cove, Figures 7-8.

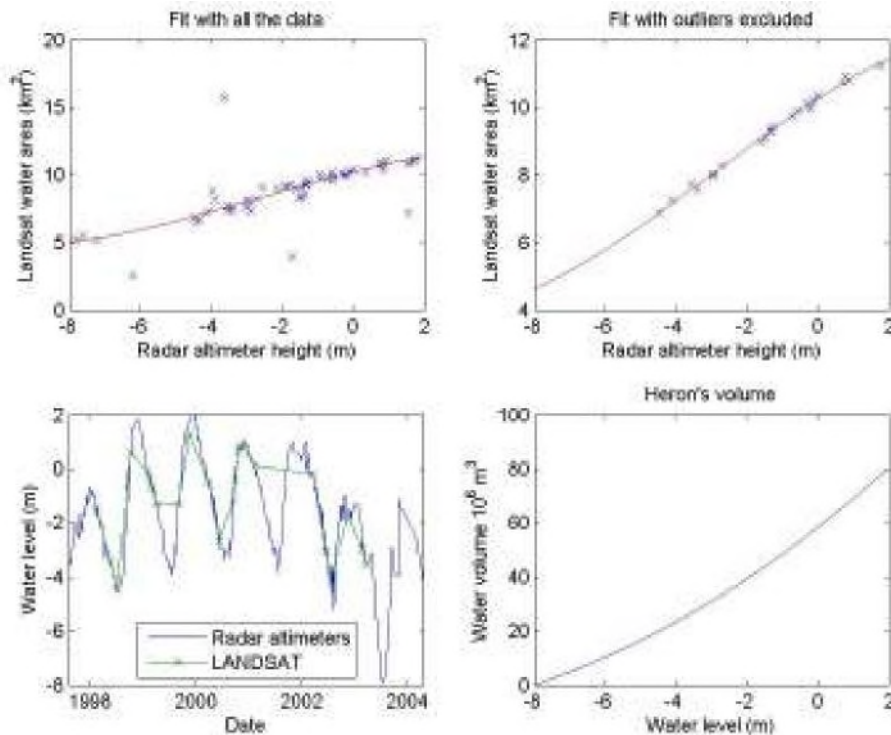


Fig. 8 Cove area inferred from Landsat vs. radar altimetry height (upper panels) and water volume from Heron's formula (lower right panel)

Movies (avi files) of the Landsat images with shoreline overlay can be downloaded from the following locations:

<http://jOmegak.com/Publications/IWTC2011/Cove.1001.avi>



It is notable that in all three cases there is a tight fit in the relationship between area and water level, with exception of a few outliers due to clouds and haze. In all three cases the area-based water levels are in very good agreement with radar altimetry. This obviously follows from the tight fit.

### 3.3 Toshka Lake results

The fact that there are an abundance of Landsat observation for 1998-2004 is most fortuitous for a study of the Toshka lakes. The period covers the entire evolution of the Toshka lakes from initial flooding of the Toshka depression in 1988, the gradual filling and expansion of the lakes through 2001, and then the long period of the lakes shrinking after 2001. This evolution is described in greater detail in (El Bastawesy [8]).

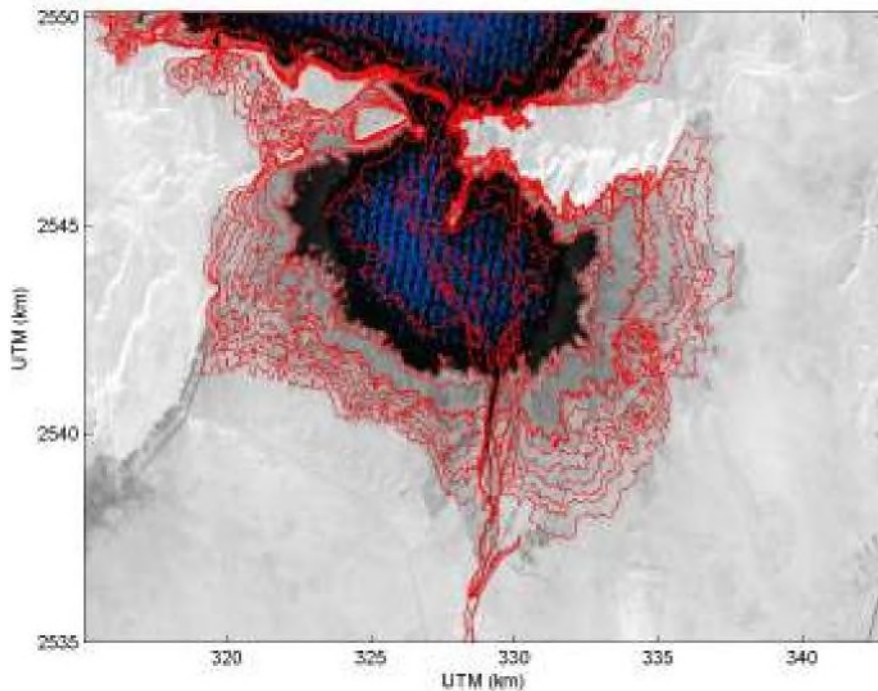


**Fig. 9 Toshka Lake 1 bathymetry 5-m contours intervals**

Figure 9 shows the area defined for Lake 1 and the bathymetric contours that will be explained later. Figure 10 compares the time series of Lake Nasser altimetry and the Lake 1 water area. Several facts are apparent from this comparison. Most notably, the Toshka area was flooded to maximum area at just the time when Lake Nasser levels reached historical maximum. Thereafter Lake Nasser levels declines and so did Toshka, but with annual cycles. Another observation is that the annual cycles in Toshka area are more abrupt than corresponding variations in Lake Nasser water levels. This is probably an indication that the draining of Lake Nasser water through the canal occurs in bursts rather than continuously.

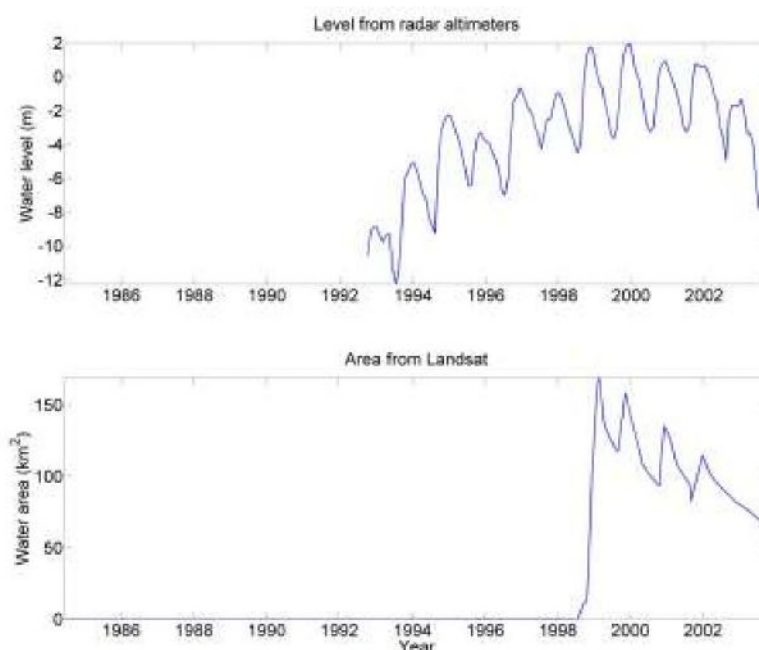


Fig. 10 Toshka Lake 1 water level (upper plot) and area (lower plot) time series

All the above observations can be better appreciated by viewing a movie of the Landsat imagery and shorelines. The movie can be downloaded from [http://jOmegak.com/Publications /IWTC2011/ToshkaLakeq.avi](http://jOmegak.com/Publications/IWTC2011/ToshkaLakeq.avi). Unfortunately, we did not have the radar altimetry data for Toshka Lakes available in time for this study so will not go into further analysis as we did with the Lake Nasser areas.

## 4. BATHYMETRY

As mentioned earlier, a bathymetry chart is a byproduct of the method. This is useful in its own right. To illustrate this potential we will discuss two types of bathymetry mappings. In one the bathymetry is from fusion of Landsat and radar altimetry. The second uses only Landsat with additional models or peg points. The method of fusing time series from both satellite types is clearly better, but it is also useful to have bathymetry when only Landsat data is available.

### 4.1 Lake Nasser bathymetry

Figure 3, 5, and 7 are the bathymetry contours derived as a byproduct of fusing Landsat shorelines and radar altimetry levels. We derive the shoreline as described in Appendix I.

### 4.2 Toshka Lake bathymetry

Since the radar altimetry was not available in time for this paper we will demonstrate a method of bathymetric mapping using only Toshka Landsat images. The method starts with the Liebe model:  $C = Const A^p$  relating water capacity,  $C$ , to water surface area  $A$ . The area is measured at some instant in time with a remote optical imagery platform such as Landsat. The coefficients  $const$  and  $p$  depend on the slope and shape of the reservoir. For reservoirs in the shape of an upside down pyramid  $p = 1.5$ . For more concave shaped reservoirs  $p$  is typically in the range of 1 to 1.4. The actual coefficients in the Liebe model were determined by adjusting to match bathymetry at two known points. We then have a relationship for  $C$  based on Landsat measured  $A$ . The water level  $L$  is estimated by.

$$L = 3 C / A$$

The resulting bathymetry is in Figure 10. The derived bathymetry is of course very approximate and the method is not completely based on remote sensing since it requires some minimal in situ data. The bathymetry in Figure 10 compares favorably with El Bastawesy [8].

## 5. CONCLUSIONS

The free availability of Landsat and radar altimeter datasets makes multi-temporal data analysis as described here practical and affordable. In this work, the approach is demonstrated on Lake Nasser with satellite data from the period 1998 to 2004. While there is further testing needed to firmly prove this technique, we believe that the initial results show a promising new approach to monitoring lakes and reservoirs worldwide.

## ACKNOWLEDGMENTS

Authors of this work wish to thank Andrea Scozzari (CNR Institute of Geosciences and Earth Resources) for the fruitful discussion and contribution to the development of this work.

## APPENDIX I - Landsat images

In this appendix we describe Landsat images and the method of measuring water surface areas. Several satellites are suitable for mapping water bodies. The moderate resolution imaging systems are the LANDSAT constellation (beginning with Landsat 4, launched 1982), SPOT constellation (begun with the first launch in 1986), and the newest and highest resolution systems IKONOS (1999), QuickBird 1 (2001), and WorldView 2 (2009).

The general approach to measuring water body areas with imaging satellites is similar for all platforms, changing in only minor details that depend mostly on the mix of spectral bands the individual platforms provide.

For the application and method discussed here the Landsat constellation has advantages that make it the clear choice above all other satellites. These are:

- A three decade of archived imagery providing a quasi regular intervals, one or two images per month, for the entire Earth;
- The greatest number of spectral bands of any of satellite platforms currently available for civilian-commercial use;
- The only satellite with high resolution short wave IR (~1.8 $\mu$ m), which we consider to be the best and easiest single band for mapping water area (as explained later);
- All data free and easily accessible by download from Internet USGS portal at <http://edcns17.cr.usgs.gov/NewEarthExplorer/>

In Landsat convention the world's surface is divided into path-row squares, each approximately 180 km x 180 km. A square can in theory be re-imaged every 16 days by each satellite in the Landsat constellation. There is then the potential for two or more images per month. In practice the available images are reduced by clouds, haze, and operational controls and priorities. One image per month is more typical of many areas of the world. When clouds are factored in one useable image per two month is typical.

The one disadvantage of Landsat relative to the other satellites mentioned is the pixel resolution. The Landsat multispectral imagery is 30m resolution. Other satellites are in the range of 2-20m. Higher resolution is important for accurate area measurement- and most important for small reservoirs, narrow channels, etc. But

higher resolution imagery comes at prohibitive cost compared to Landsat and in any case are not available with the temporal frequency and historical record of Landsat, so the issue of resolution is mute. Furthermore there are algorithmic tricks to increase the effective resolution from Landsat. One well known method, pan-sharpening, combines the multispectral bands (30m) with the Panchromatic (15 m) to achieve effective 15 m resolution. Another method, pixel unmixing, has the potential for even higher effective resolution.

Water area is generally darker than surrounding land so one commonly used method to mapping water areas, with Landsat and other imaging satellites, is based on an intensity threshold. Water surface area is the count of the number of image pixels below the threshold. This can be done with any of the Landsat multi-spectral bands, and even with the panchromatic image.

This simple threshold method, however, will tend to underestimate the water area because there is some fuzziness in land-water separation near the shoreline, tending to push the shoreline out. Our water area algorithm incorporates the following four considerations and improvements to overcome the fuzziness effects.

- (1) Reflection of sun and sky light from the water surface. This is especially significant when wind is roughening the surface or specular sun reflection is present. We eliminated these factors by taking radiance from a relatively deep area (determined by a separate algorithm) as a reference radiance. This reference is subtracted from all pixels as a first step in water-land classification. This should, in absence of other effects, discussed below, set all water pixels to near zero.
- (2) The adjacency effect (Liang et al. [9]). Atmospheric scattering spreads land radiance over adjacent water body. The water pixel radiances are then not zero (after water reflection correction mentioned above) and the land-water boundary is less distinct. We use a simple approximation of traditional adjacency correction methods (see (Liang et al. [9]) for review and further references). A first estimate of the shoreline pixels is made. Those pixel that lie on the shoreline are presumably a mix of land and water. The intensity in the water pixels nearest the shoreline, but not including the shoreline pixels, is taken as a first estimate the adjacency radiance. This intensity is subtracted from cells on and adjacent to the first shoreline estimate. The shoreline is estimated again, now with the first order estimate of adjacency radiance removed. The second shoreline always encompasses a slightly larger water areas. This process can be repeated for another iteration. We see the effectiveness of this approach most notably in narrow water inlets and rivers where land surrounds the water pixels on two or even three sides.
- (3) Bottom reflected radiance. In green-blue, and to a lesser but not negligible degree in red and near IR, there is sufficient radiance propagating through the water column and then reflected from the bottom back up to the sensor. This reflection further dilutes the land-water contrast. It can also be confused with the adjacency effect. In the present analysis we choose to use only the short-wave IR where water attenuation is much greater than in the visible and near IR bands. We can thus ignore bottom reflection and assume that all the over water radiance if any is due to adjacency. As previously mentioned, one advantage of Landsat is its short wave IR band - available from no other satellite.
- (4) Unresolved mixture of land and water on shoreline. It is possible to get more accurate water area measurement by estimating the fraction of each shoreline pixel that is water. As mentioned before, the common techniques are pan sharpening and pixel spectral unmixing. For our application the unmixing approach is more useful. Unmixing methods can use multiple spectral bands but are especially easy to calculate when there is only ones spectral band, namely the short-wave IR. The radiance from water surface is zero by definition (after correcting for adjacency). For land the radiance is some value X, which we estimate from immediate adjacent land pixels. The radiance of shoreline pixels, between 0 and X, is thus indicative of the fraction of the cell area that is land. We accumulate these fractional pixel water areas in our total for the water body surface area.

## APPENDIX II - Space based Radar Altimeters

In this appendix we describe radar altimetry and the method of measuring water levels.

Radar altimetry is an important technique for sensing water levels from space (Fu and Cazenave [10]). It is just a more complicated tide gauge with the difference that the altimeter-derived measurements are an average over a footprint with much lower revisiting time. The launch of TOPEX/Poseidon satellite mission in 1992 provided the greatest impetus for radar altimetry research in the 20th century. Its launch was followed by Jason-1 (2001) and Jason-2 (2008). ESA satellites were launched in 1991, 1995, 2002 (ERS-1, ERS-2, Envisat) and 2010 (CryoSat-2). US Navy Geosat Follow-On was launched on 1998. Whilst several of these missions are still flying and expected to continue operation for the foreseeable future, new missions are planned to be launched over the next few years (HY-2, AltiKa, Sentinel-3, SWOT). A global record of 18 years of raw data from a series of radar altimetry missions is presently available and represents a unique resource for retrospective analysis in all water bodies.

The raw data provided by the altimeter do not come ready for use. A complex sequence of processing steps is usually necessary to transform these raw data into usable water level information. These steps essentially consist of removing unwanted effects caused by the instrument, atmosphere and ocean (Chelton et al. [11]). The official products (e.g., AVISO, RADS) generally contain sensor measurements, orbit estimations and a full set of corrections, with average measurements typically at 1 Hz or ~7 km along track. This degree of resolution is normally sufficient for studies of big water bodies.

Radar altimetry faces some technical challenges in smaller water bodies. These are well identified and described in Vignudelli et al. [1]. Some examples include the retracking of the raw ocean return signals (waveforms) in the last 10 kilometers next to the land and the inadequacy of some open ocean corrections (e.g., for path delay due to the wet troposphere within 50 km; for atmospheric effects due their more complex variability). These and other specific problems (e.g., reference frame for data collocation, editing strategy) make it difficult to take data from official products using standard processing and get results comparable to those from open ocean.

The importance of radar altimetry in the inland waters has been recognized through a series of projects aiming at developing a global data base of enhanced altimeter-derived estimates of water levels in this domain. The most important initiatives are:

- HYDROWEB (LEGOS) – (<http://www.legos.obs-mip.fr/en/soa/hydrologie/hydroweb/>);
- River & Lakes (ESA) - (<http://earth.esa.int/riverandlake/>);
- PECAD (USDA) (<http://www.pecad.fas.usda.gov/>)

The water levels from Hydroweb (LEGOS) are based on merged TOPEX/Poseidon, Jason, ENVISAT and Geosat Follow-On data provided by ESA, NASA and CNES data centers. The altimeter range measurements used to estimate those water levels consist of 1Hz data. All classical corrections (orbit, ionospheric and tropospheric corrections, polar and solid Earth tides and sea state bias) are applied. If different satellites cover the same water body, the water level is computed in a three-step process. Each satellite data set is processed independently. Potential radar instrument biases between different satellites are removed using TOPEX/Poseidon data as reference. Then water levels from the different satellites are merged on a monthly basis as the revisiting cycles vary from 10 days for TOPEX/Poseidon and Jason, to 17 days for Geosat Follow-On and 35 days for ERS and Envisat. Examples of applications of water levels from Hydroweb can be found in Crétaux et al. [12].

On the other hand, water levels from PECAD (USDA) are based on one satellite (TOPEX/Poseidon) on a 10 day basis. The altimeter range measurements used to estimate those water levels consist of 1Hz data. All classical corrections are applied. Major details can be found in Birkett et al. [13].

## REFERENCES

- [1] Vignudelli, S., Kostianoy, A.G., Cipollini, P. and Benveniste, J. (Ed.), *Coastal Altimetry*, Springer-Verlag Berlin Heidelberg, doi:10.1007/978-3-642-12796-0, pp. 578, 2011.
- [2] Liebe, J.R., *Estimation of Water Storage Capacity and Evaporation Losses of Small Reservoirs in the Upper East Region of Ghana*, Diploma thesis, Faculty of Mathematics and Natural Sciences, University of Bonn, Germany, pp. 106, 2002.
- [3] UNESCO, *Application of satellite remote sensing to support water resources management in Africa: Results from the TIGER Initiative*, Technical Documents in Hydrology, n. 85, UNESCO, Paris, pp. 153, 2010.
- [4] Taube, C.M., *Instructions for winter lake mapping*, in *Manual of fisheries survey methods II: with periodic updates*, (Ed. Schneider, J.C.), State of Michigan, Department of Natural Resources, Fisheries Special Report, N. 25, Chapter 11, 1-8, 2000.
- [5] Mason, D.C., Davenport, I.J., Flather, R.A., McCartney, B. and Robinson, G.R., Construction of an intertidal digital elevation model by the 'water-line' method", *Geophysical Research Letters*, vol. 22, pp. 3187-3190, 1995.
- [6] Yamano, H., The use of multi-temporal satellite images to estimate intertidal reef-flat topography, *Journal of Spatial Science*, 52, 71-77, 2007.
- [7] Ismail, M., Yakoub N.G.R. and Farag, F., Toward Sustainable Development in Toshka Region: Development of a Geo-Information System Using Remote Sensing and GIS, [http://www.mes.eg.net/acrobat\\_files/3\\_5.pdf](http://www.mes.eg.net/acrobat_files/3_5.pdf), 2005.
- [8] Bastawesy M., El Arafat, S., Khalaf F. (2007). Estimation of water loss from Toshka Lakes using remote sensing and GIS, *Proc. 10th AGILE International Conference on Geographic Information Science*, Aalborg University, Denmark, pp.1-9 (in Cd-Rom), 2007.
- [9] Liang, S., Fang, H. and Chen, M., *Atmospheric correction of Landsat ETM+ land surface imagery. I. Methods*, IEEE Transactions on Geoscience and Remote Sensing, 39, 11, pp. 2490-2498, 2001.
- [10] Fu, L.L. and Cazenave, A. (Ed.), *Satellite altimetry and Earth sciences, A Handbook of techniques and applications*, International Geophysics Series, 69, Academic Press, San Diego, pp. 463, 2001.
- [11] Chelton, B., Ries, J., Haines, B.J., Fu, L.L. and Callahan P.S., Satellite altimetry. in *Satellite Altimetry and Earth Sciences: A handbook of techniques and Applications*, (Ed. Fu L.L. and Cazenave A.), International Geophysics Series, 69, Academic Press, San Diego, pp. 1-131, 2001.
- [12] Crétaux, J.F., Calmant, S., Abarca del Rio, R., Kouraev, A., Bergé-Nguyen, M. and Maisongrande, P., Lakes Studies from Satellite Altimetry, in *Coastal Altimetry* (Ed. Vignudelli S., Kostianoy A.G., Cipollini P. and Benveniste J.), , Springer-Verlag Berlin Heidelberg, pp. 509-533, doi:10.1007/978-3-642-12796-0\_19, 2011.
- [13] Birkett, C., Reynolds, C., Beckley, B. and Doorn, B., From Research to Operations: The USDA Global Reservoir and Lake, in *Coastal Altimetry* (Ed. Vignudelli S., Kostianoy A.G., Cipollini P. and Benveniste J.), , Springer-Verlag Berlin Heidelberg, pp. 19-50, doi:10.1007/978-3-642-12796-0\_2, 2011.